6-1-1964

On The Solar Magnetic Field In Inter-Planetary Space

Jacqueline H. Hill

ON THE SOLAR MAGNETIC FIELD IN INTERPLANETARY SPACE

By

Jacqueline H. Hill

A Thesis

Submitted in Partial Fulfillment of the

Requirements for the Degree of

Master of Science in Physics

The University of New Mexico

1964

This thesis, directed and approved by the candidate's committee, has been accepted by the Graduate Committee of the University of New Mexico in partial fulfillment of the requirements for the degree of

MASTER OF SCIENCE

Dean

6/1/64
Date

ON THE SOLAR MAGNETIC FIELD IN INTERPLANETARY SPACE

Jacqueline H. Hill

Thesis committee

Chairman

ACKNOWLEDGMENTS

I would like to express my appreciation to Dr. Roy Thomas for consultation on the theoretical portion of this thesis, in particular for suggesting the mathematical formulations which led to magnetic fields II and V; to Betty P. Phelan, Ronald C. Ericksen, and Charles E. Williams, for technical assistance; and to Dr. Victor H. Regener for suggesting the problem, and for help during its progress.

TABLE OF CONTENTS

LIST OF TABLES

LIST OF FIGURES

CHAPTER I

INTRODUCTION

The purpose of this thesis is to determine, experimentally and theoretically, an axially symmetric current distribution which would simulate the currents believed to flow in interplanetary space around the sun. The general magnetic field of the sun is assumed to originate as a dipole field which induces currents in the plasma of the solar atmosphere. The dipole field is in turn modified by the induced currents. This phenomenon is often described in terms of a diamagnetism of the plasma. In the limiting case, this diamagnetism would almost completely prevent the inducing field from penetrating the plasma.

Experimentally, the induced current distribution is simulated by a large number of co-planar concentric circular conductors carrying individually adjustable currents. By trial and error, a current distribution was found which produced in the plane of the currents a magnetic field equal to that of a dipole oriented normal to the plane at its center. This inverse-cube magnetic field is then superimposed upon the dipole field such that

the two fields cancel in the plane, as though the induced currents flowed in a perfectly diamagnetic sheet. This diamagnetic sheet is identified with the equatorial plane of the sun, and the plot of the vector sum of the experimental and the dipole fields at points away from the plane is then assumed to furnish a rough approximation to the behavior of the actual solar magnetic field.

In the theoretical portion of the thesis, axially symmetric current distributions flowing in space rather than in a plane are postulated, and the resulting magnetic fields are discussed. In particular, this thesis investigates the possibility that the solar magnetic field might supply a centripetal force capable of producing co-rotation of the solar atmosphere with the sun itself, deep into interplanetary space.

CHAPTER II

THE EXPERIMENTAL FIELD

The conducting rings which produce the experimental current distribution are printed onto a circuit board, as shown schematically in Figure 1. The individual circuits shown in Figure 2 are connected in series, one for each conducting ring. The current in each ring is determined by the series resistor R_1 and the variable shunt resistance R_2.

Originally, power was supplied by a D. C. power supply, and the current was pulsed with a mercury switch driven by an oscillator. Later, as larger currents were desired, the power input system shown in Figure 3 was used. The currents in the rings are pulsed in both cases, so that a pickup coil could be used to obtain measurements of the relative field intensity. The currents are measured by means of an oscilloscope connected across R_1.

The magnetic field obtained using the mercury switch is plotted in the equatorial plane in Figure 4. The radius r_o, beyond which the experimental field assumes the $1/r^3$ dipole-field behavior, is identified with the solar radius. The radius R, the position of the maximum

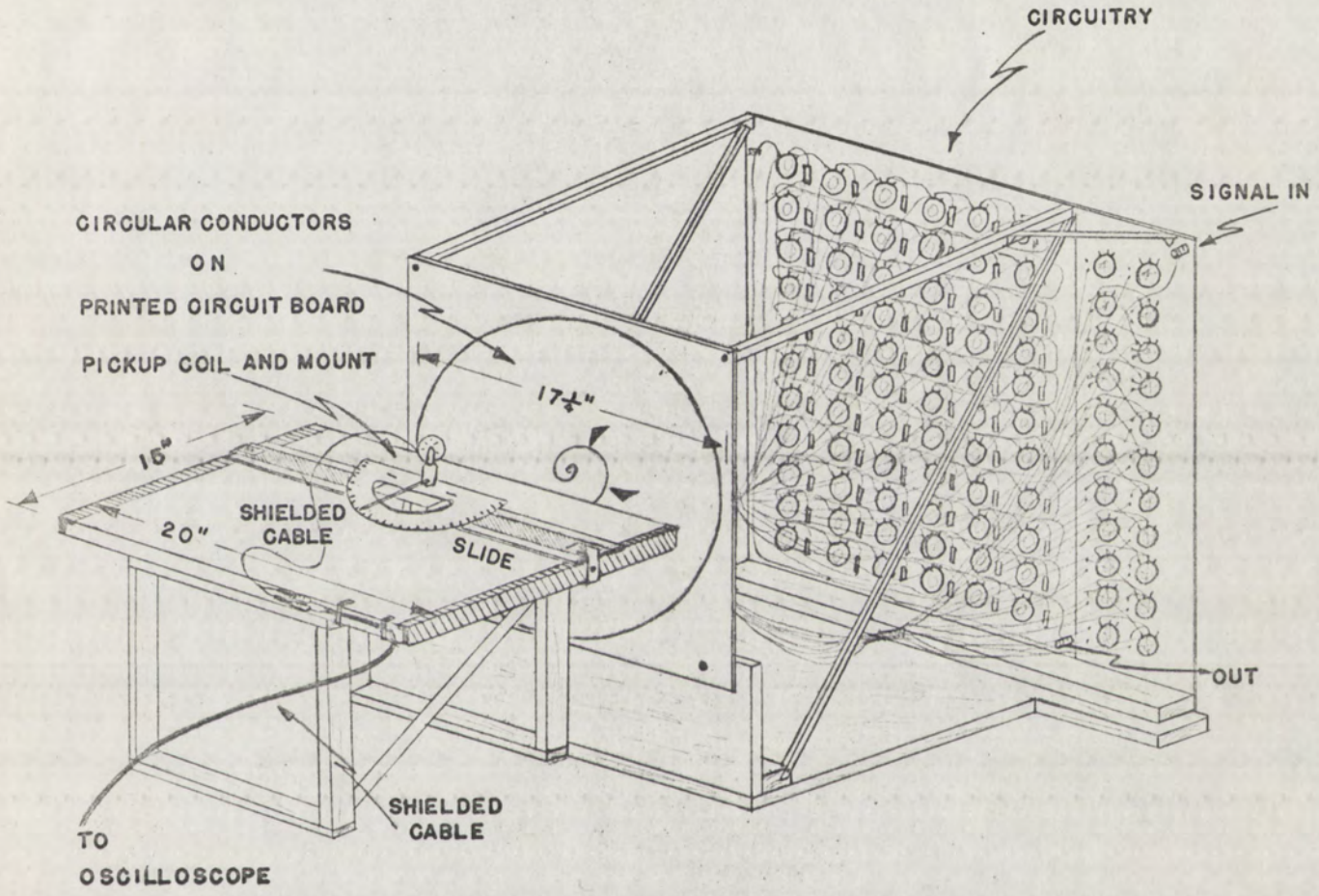

FIGURE 1
EXPERIMENTAL APPARATUS

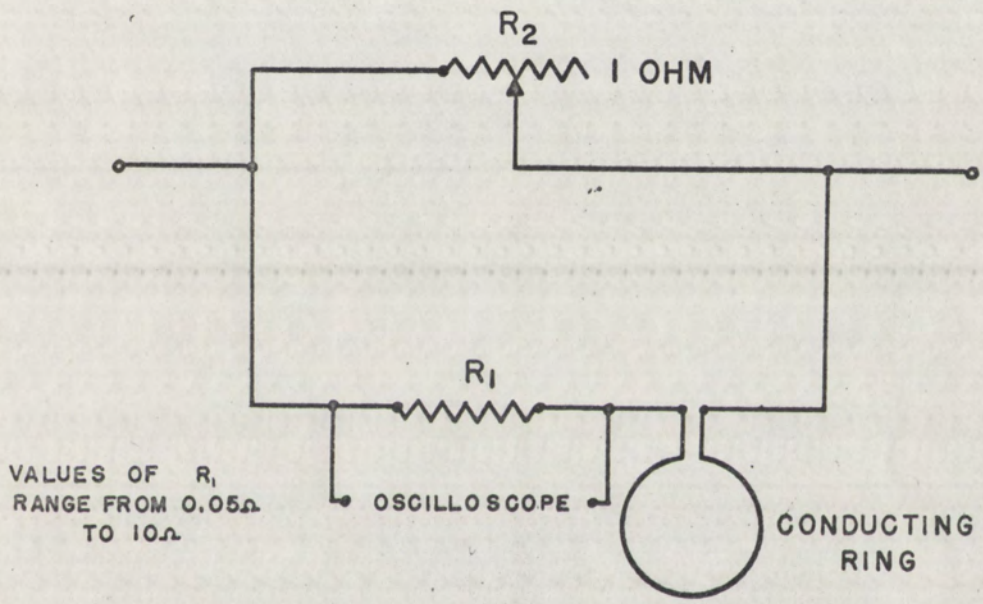

FIGURE 2

CIRCUITRY OF CONDUCTING RINGS

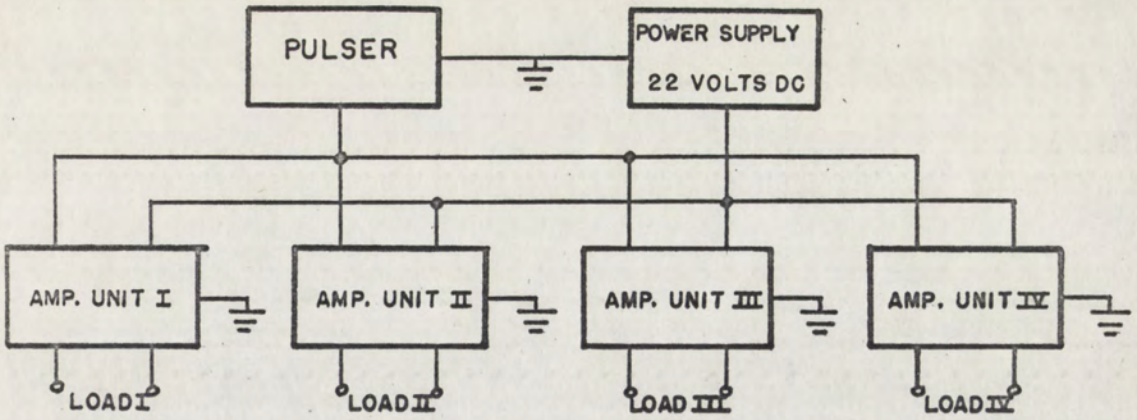

a. POWER SUPPLY

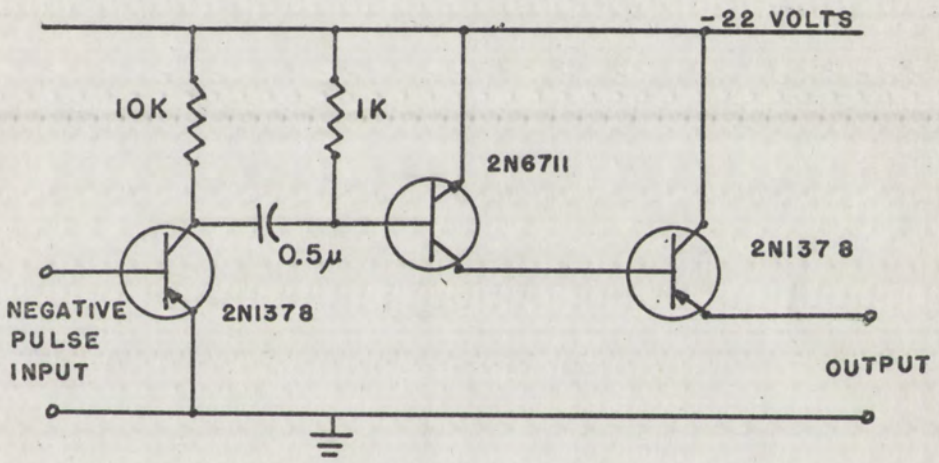

b. CIRCUITRY OF AMPLIFIER UNITS I-IV

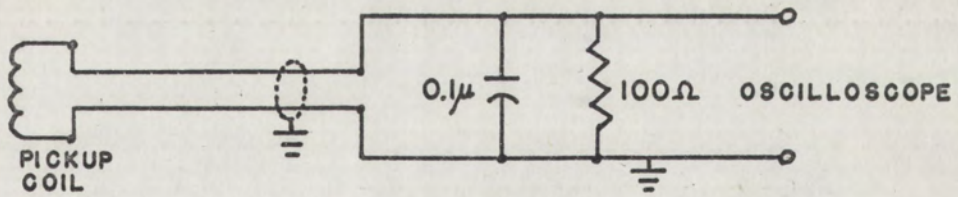

c MEASUREMENT OF MAGNETIC FIELD

FIGURE 3

FINAL POWER SUPPLY AND FIELD MEASUREMENT SYSTEMS

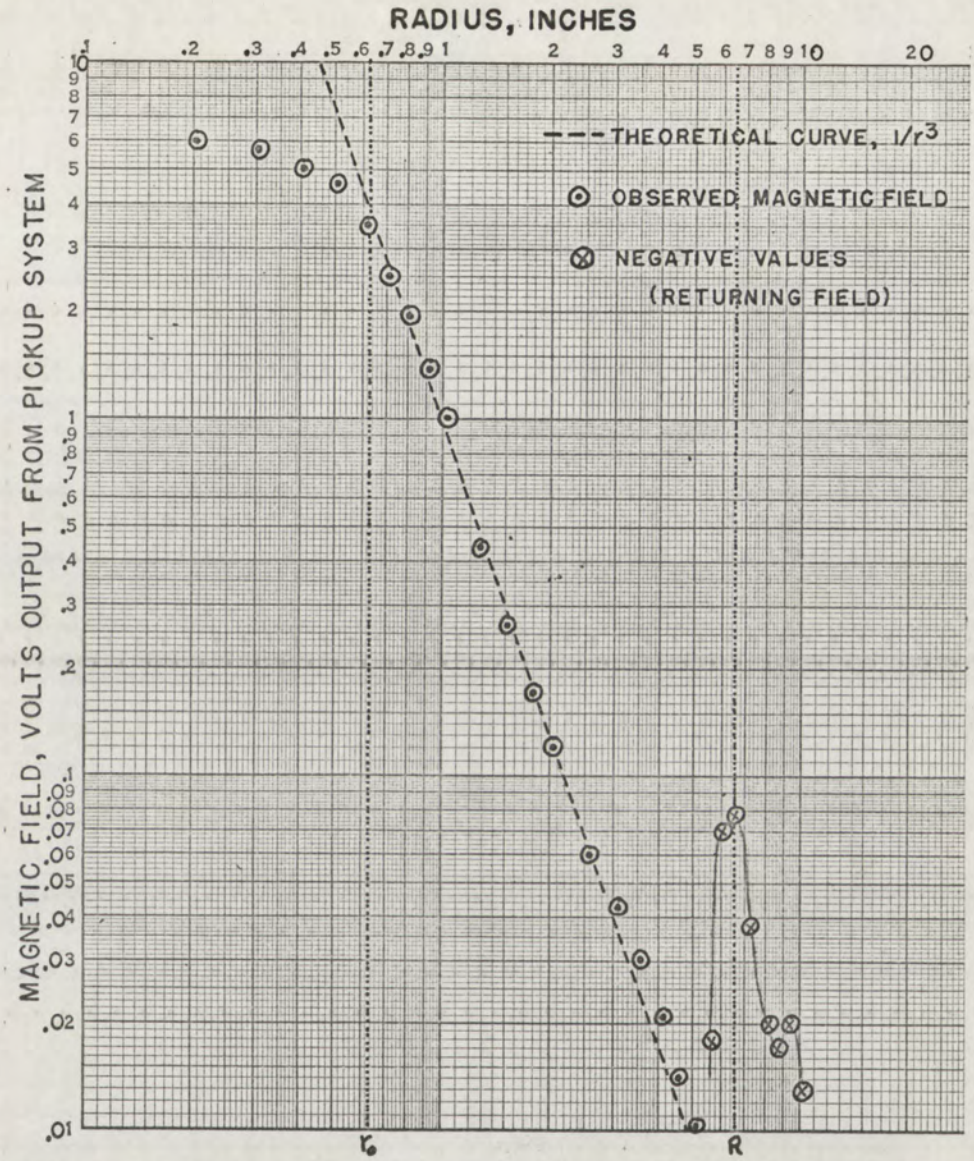

FIGURE 4

MAGNETIC FIELD IN THE EQUATORIAL PLANE FOR PLASMA EXTENDING 10 SOLAR RADII

returning field, is assumed to correspond roughly to the radius of the plasma sheet. It is clear from Figure 4 that in this case the plasma sheet extends only as far as about 10 solar radii.

Gravitational attraction in itself can be expected to produce co-rotation of the solar atmosphere out to 40 solar radii, which is the radius of the "synchronous" orbit around the sun. Thus, it was desired to produce a model in which the plasma extends to 40 solar radii or beyond.

Using the circuitry shown in Figure 4, the plasma was extended to 20 solar radii. It proved impractical if not impossible to improve upon this. One is limited in extending the dipole behavior to larger radii on the board because the magnetic field necessarily becomes small beyond the point of practical measurement. In particular, the signal from the pickup coil approaches the level of pickup from stray fields. Also, relative phase shifts in the signal from thedifferent portions of the circuit board prevent a clean zero at the point where the field inverts. It is difficult to bring the $1/r^3$ field closer to the center of the sheet, for in this region the difference in the current from one ring to the next is large, and the system can no longer be treated as a uniform "current

sheet." The field strength also changes rapidly in this region, and the finite size of the pickup coil interferes with an accurate determination of the field intensity.

Figure 5a shows the experimental field which corresponds to a plasma sheet extending to 20 solar radii. The linear density of lines is drawn proportional to the square root of the field intensity H, since H is a measure of the surface density of magnetic lines of flux. The dipole field, drawn to the same scale, is shown in Figure 5b, and Figure 5c shows the vector sum of the experimental and dipole fields. Near the poles, the total field has a tendency to become more radial than the original dipole field. There is some correspondence here with observations made during solar eclipses of the "polar plumes," coronal streamers issuing from the polar regions of the sun.

The linear current density producing this field, shown in Figure 6, decreases over most of its extent as the inverse square of the radial distance from the center of the sheet.

Although the final magnetic field (Figure 5c) encloses a plasma extending to only 20 solar radii, information concerning a plasma at 40 solar radii can be estimated by extrapolation. The maximum edge field

FIGURE 5a

EXPERIMENTAL MAGNETIC FIELD

DISTANCE FROM CURRENT SHEET, INCHES

RADIAL DISTANCE, INCHES

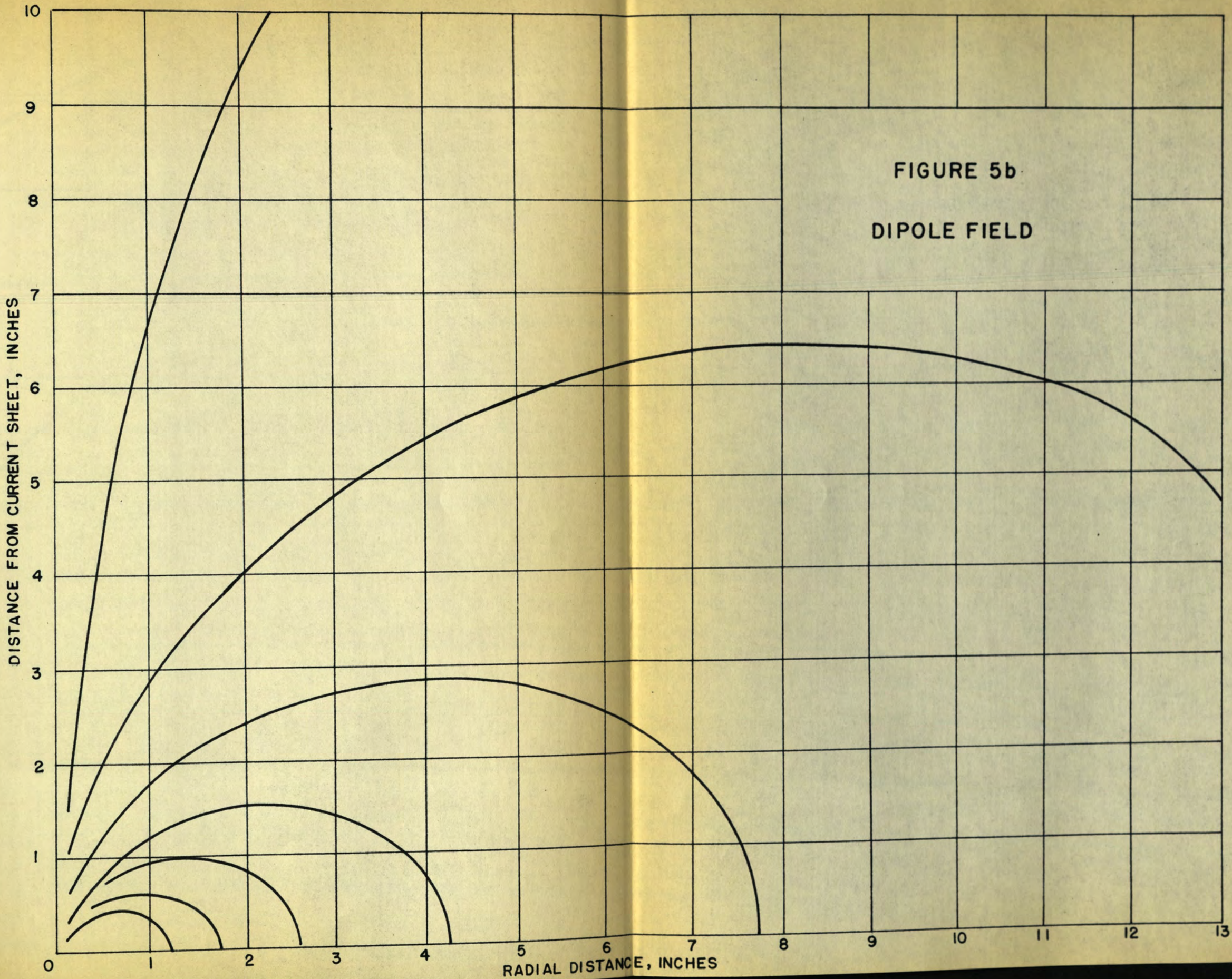
FIGURE 5b
DIPOLE FIELD
DISTANCE FROM CURRENT SHEET, INCHES
RADIAL DISTANCE, INCHES
0
1
2
3
4
5
6
7
8
9
10
11
12
13

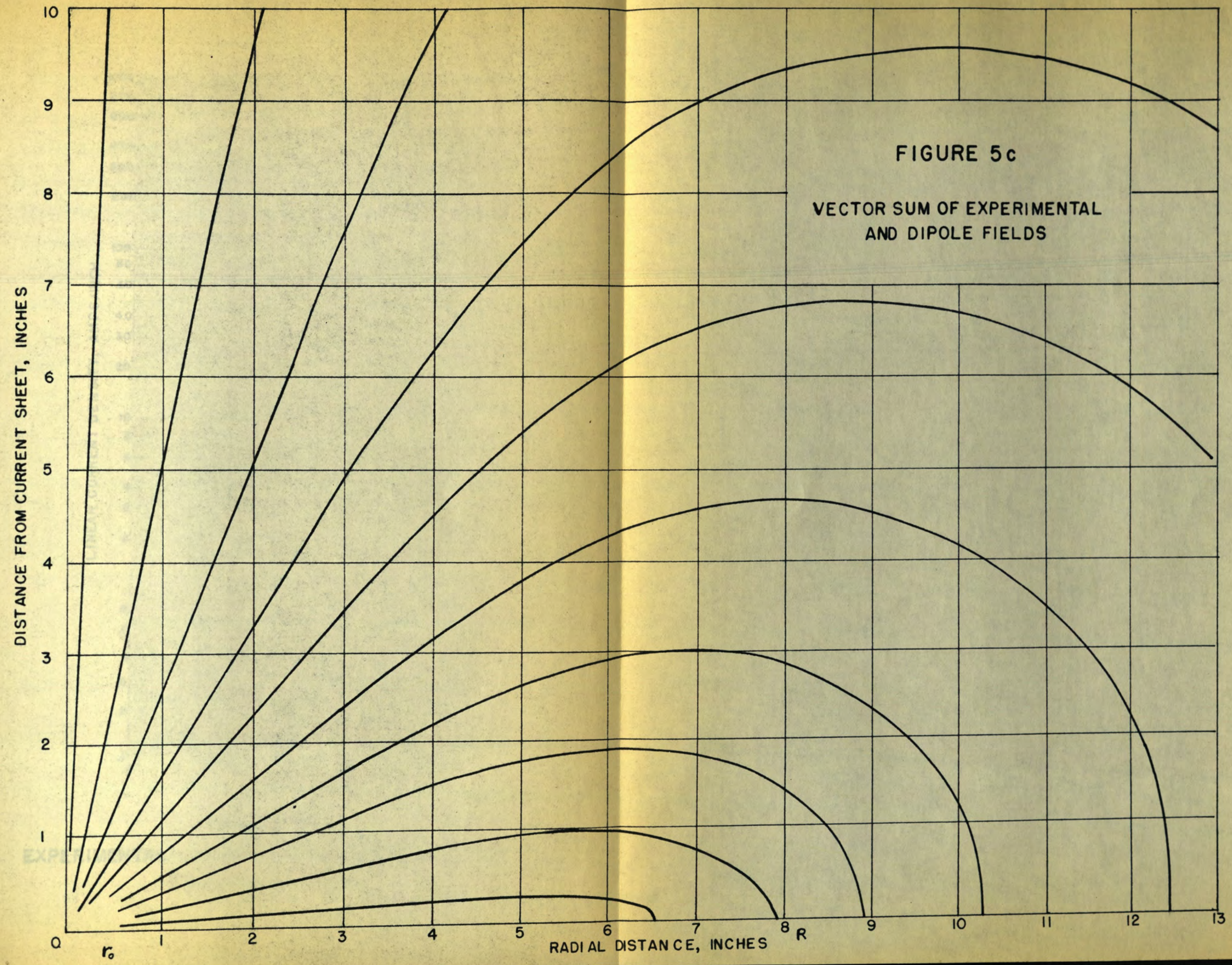
FIGURE 5c
VECTOR SUM OF EXPERIMENTAL AND DIPOLE FIELDS
DISTANCE FROM CURRENT SHEET, INCHES
RADIAL DISTANCE, INCHES
0
r_o
R
1
2
3
4
5
6
7
8
9
10
11
12
13

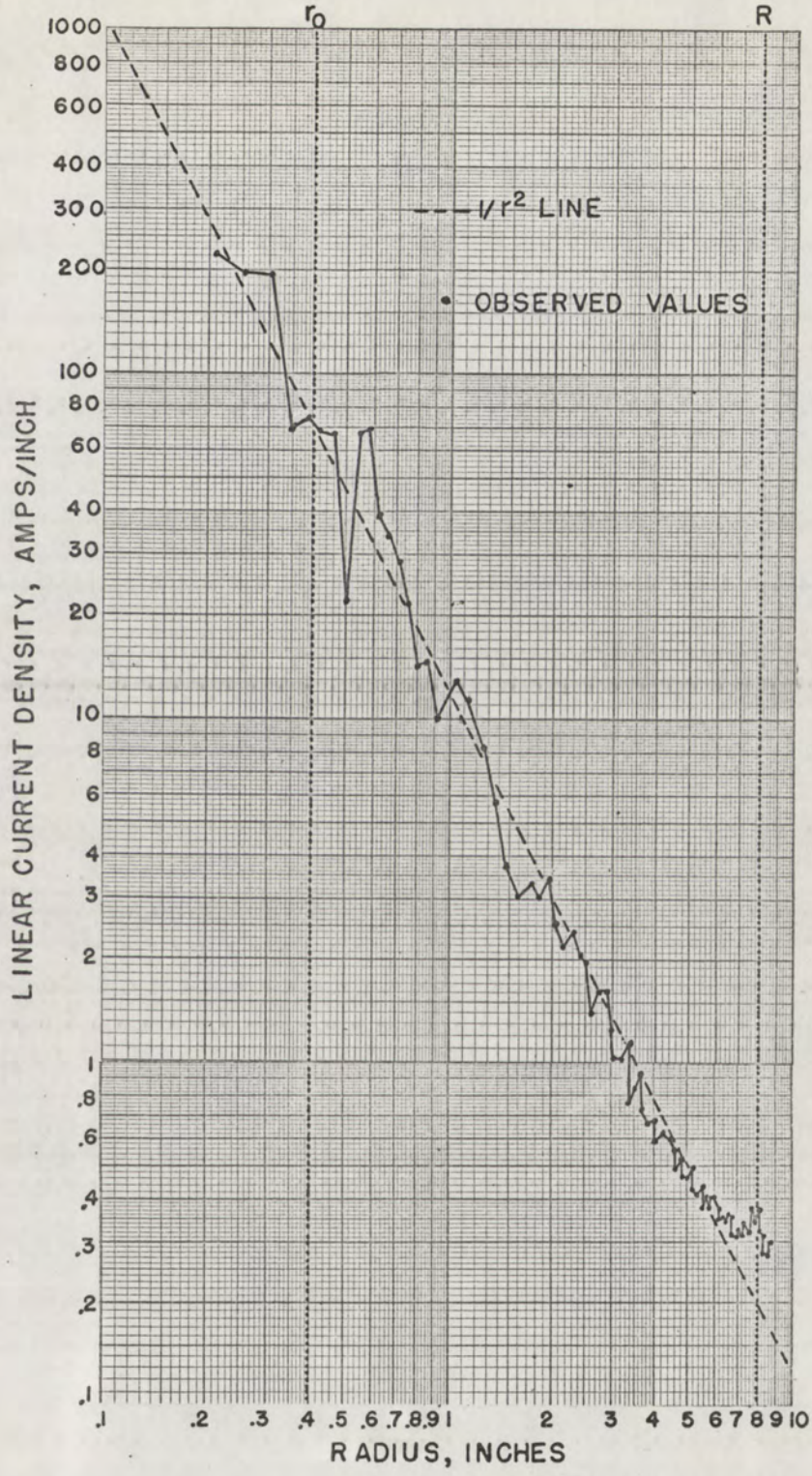

FIGURE 6

EXPERIMENTAL LINEAR CURRENT DENSITY IN THE EQUATORIAL PLANE

enclosing a plasma at 10 solar radii (Figure 4) is 15 times larger than that of the dipole field alone; the plasma extending to 20 solar radii is enclosed by a field 32 times as large as the dipole field. Therefore, a maximum edge field 64 times larger than the dipole field was assumed to bound a plasma extending 40 solar radii into space. Assuming a solar (dipole) field of 1 gauss at the poles, the field strength of the maximum edge field is found to have the values shown in Table I.

TABLE I

MAXIMUM EDGE FIELD IN THE EQUATORIAL PLANE

R, Plasma boundary in solar radii	Dipole field, gauss	Maximum edge field (dipole plus induced field,) gauss
10	5.0×10^{-4}	7.5×10^{-3}
20	6.2×10^{-5}	2.0×10^{-3}
40 (EXTRAPOLATED)	7.8×10^{-6}	5.0×10^{-4}

The pressure $H^2/8\pi$ exerted by the magnetic field on the boundary of the plasma at 40 solar radii in the equatorial plane is thus 10^{-8} dynes/cm^2. Assuming an ideal gas at the constant temperature $T = 10^6$ degrees for the corona, the particle pressure at the same point is about $nkT = 1.6 \times 10^{-6}$ dynes/cm^2, where n is the number density of electrons and protons in the equatorial plane.[1]

On the basis of this very crude determination, it was concluded that particle and magnetic pressures at 40 solar radii are almost equal, and that co-rotation of the solar atmosphere could not take place much beyond this radius. A more accurate analysis would have required that a model be built in which the plasma extends to 40 solar radii, and that the curvature of the lines of force be taken into account. This was not done in order to proceed with the entirely theoretical approach which follows.

---

[1] Values of the number density of electrons in the equatorial plane were calculated by Mr. Martin Tierney, assuming a uniformly rotating plasma of constant temperature 10^6 degrees and of density 1.8×10^8 electrons/cm^3 at the base of the corona. It is also assumed that the equatorial plane is field-free, and that the magnetic field immediately on either side is parallel to the plane.

CHAPTER III

THEORETICAL CURRENT DISTRIBUTIONS

Since it is impractical to construct a volume current distribution experimentally, hypothetical induced fields and spatial current distributions with axial symmetry were investigated. In the formulations which follow, a certain behavior was postulated for one component of the magnetic field. The other component was then determined by setting up the divergence condition:

$$\text{Div } \vec{H} = 0. \tag{1}$$

When applicable, the boundary condition that the θ component of H (spherical coordinates) vanish at $\theta = 0$ was imposed. The current distribution producing such a field is then determined by Maxwell's relation,

$$\text{Curl } \vec{H} = 4\pi j. \tag{2}$$

The first model postulates the magnetic field components

$$H_r = \frac{2H_o}{\pi}\left(\frac{r}{R}\right)^{-2} e^{-\left(\frac{r}{R}\right)^2}\left[\left(\theta - \frac{\pi}{2}\right) - \sin\theta\cos\theta\right], \tag{3a}$$

and

$$H_\theta = \frac{4H_o}{\pi} e^{-\left(\frac{r}{R}\right)^2}\left[1 - \frac{1}{3}\sin^2\theta - \frac{\left(\theta - \frac{\pi}{2}\right)\cos\theta + \frac{\pi}{2}}{\sin\theta}\right]. \tag{3b}$$

This field, shown in Figure 7, is more radial near the

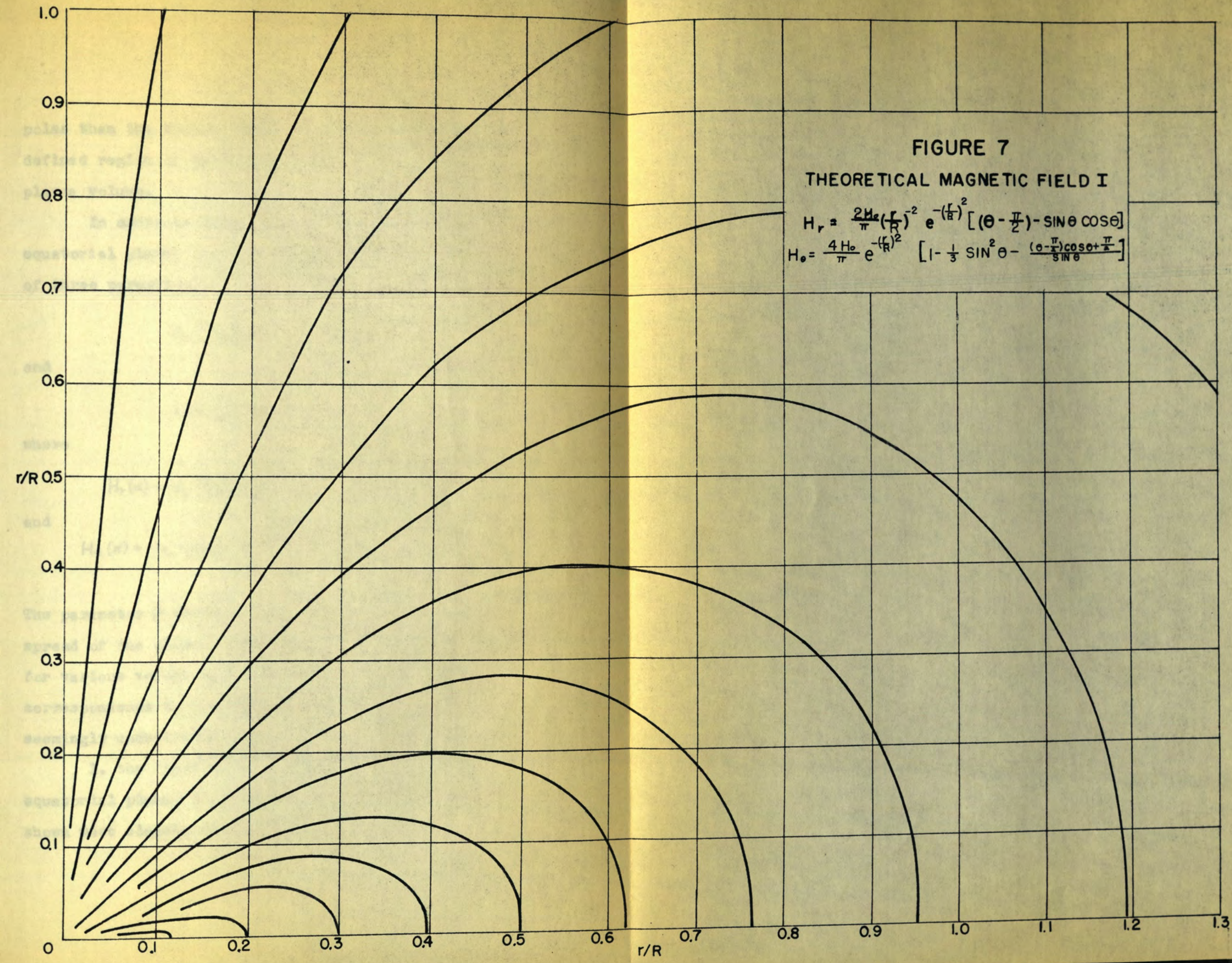

FIGURE 7

THEORETICAL MAGNETIC FIELD I

$$H_r = \frac{2H_o}{\pi}\left(\frac{r}{R}\right)^{-2} e^{-\left(\frac{r}{R}\right)^2}\left[\left(\theta - \frac{\pi}{2}\right) - \sin\theta\cos\theta\right]$$

$$H_\theta = \frac{4H_o}{\pi} e^{-\left(\frac{r}{R}\right)^2}\left[1 - \frac{1}{3}\sin^2\theta - \frac{\left(\theta - \frac{\pi}{2}\right)\cos\theta + \frac{\pi}{4}}{\sin\theta}\right]$$

poles than the dipole field, but it lacks the clearly defined region of zero field which should represent the plasma volume.

In order to introduce a void volume in the equatorial plane, the next model was written in terms of three parameters:

$$H_r = H_r(\alpha_1) - H_r(\alpha_2), \tag{4a}$$

and

$$H_\theta = H_\theta(\alpha_1) - H_\theta(\alpha_2), \tag{4b}$$

where

$$H_r(\alpha) = H_o \frac{\cos\theta}{\alpha}\left(\frac{r}{R}\right)^{-2} e^{-\alpha\left(\frac{r}{R}\right)^2} e^{-\beta\cos^2\theta}, \tag{5a}$$

and

$$H_\theta(\alpha) = H_o \frac{1}{\beta \sin\theta} e^{-\alpha\left(\frac{r}{R}\right)^2}\left[e^{-\beta\cos^2\theta} - e^{-\beta}\right]. \tag{5b}$$

The parameter β serves as a measure of the angular spread of the plasma. Mappings of this magnetic field for various values of β (Figure 8) show a certain correspondence to the experimental results. Two seemingly undesirable properties are noted, however:

1. the field strength inside the plasma (off the equatorial plane) is greater than that outside, as shown most clearly by Figure 8b;

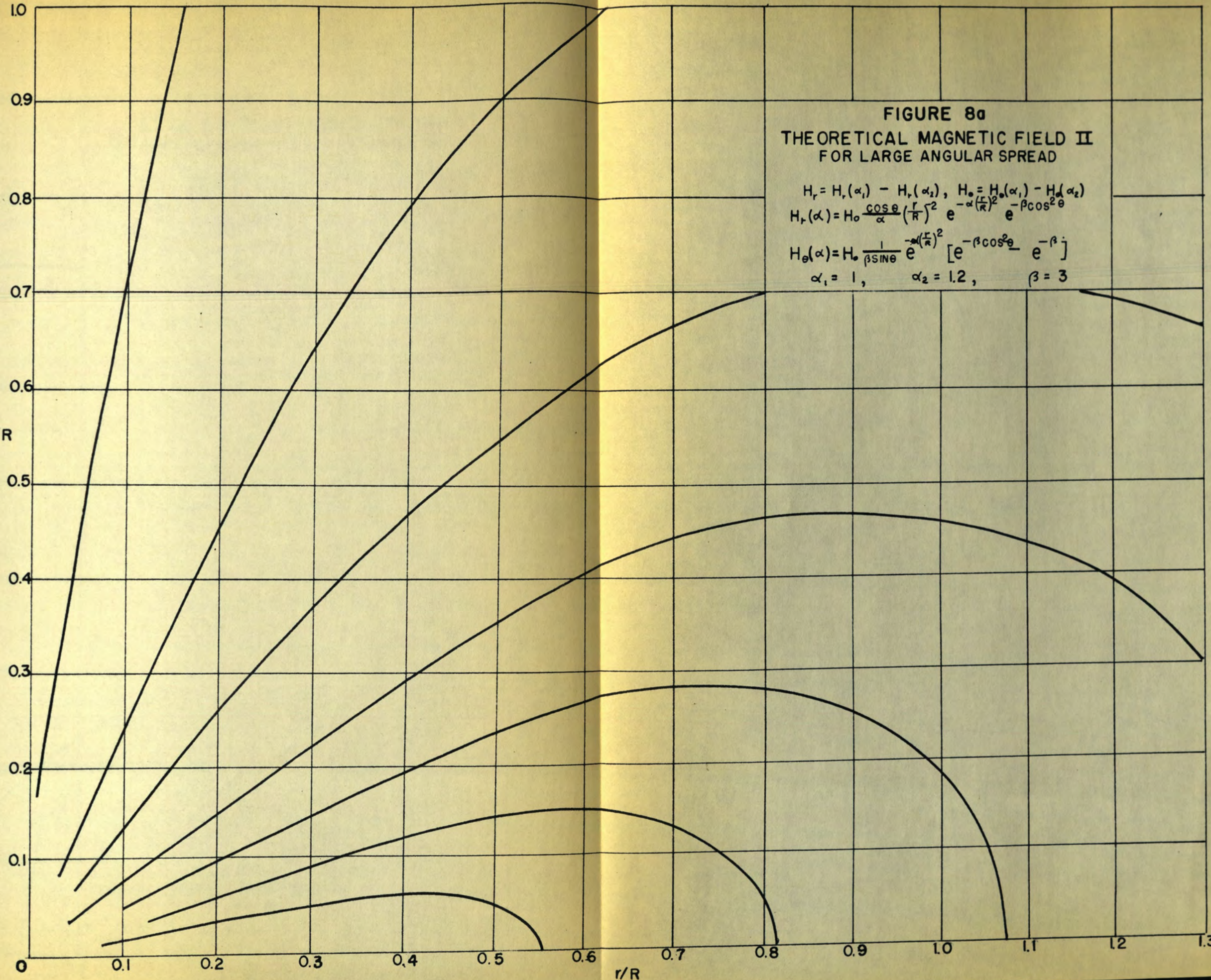

FIGURE 8a

THEORETICAL MAGNETIC FIELD II
FOR LARGE ANGULAR SPREAD

$$H_r = H_r(\alpha_1) - H_r(\alpha_2), \quad H_\theta = H_\theta(\alpha_1) - H_\theta(\alpha_2)$$

$$H_r(\alpha) = H_o \frac{\cos\theta}{\alpha}\left(\frac{r}{R}\right)^2 e^{-\alpha\left(\frac{r}{R}\right)^2} e^{-\beta\cos^2\theta}$$

$$H_\theta(\alpha) = H_\theta \frac{1}{\beta \sin\theta} e^{-\alpha\left(\frac{r}{R}\right)^2}\left[e^{-\beta\cos^2\theta} - e^{-\beta}\right]$$

$\alpha_1 = 1, \quad \alpha_2 = 1.2, \quad \beta = 3$

FIGURE 8b

THEORETICAL MAGNETIC FIELD II
FOR SMALL ANGULAR SPREAD

$H_r = H_r(\alpha_1) - H_r(\alpha_2)$, $H_\theta = H_\theta(\alpha_1) - H_\theta(\alpha_2)$

$H_r(\alpha) = H_o \frac{\cos\theta}{\alpha} \left(\frac{r}{R}\right)^{-2} e^{-\alpha\left(\frac{r}{R}\right)^2} e^{-\beta\cos^2\theta}$

$H_\theta(\alpha) = H_o \frac{1}{\beta \sin\theta} e^{-\alpha\left(\frac{r}{R}\right)^2} \left[e^{-\beta\cos^2\theta} - e^{-\beta}\right]$

$\alpha_1 = 1$, $\alpha_2 = 1.2$, $\beta = 3$

PLASMA BOUNDARY

r/R

1.0
0.9
0.8
0.7
0.6
0.5
0.4
0.3
0.2
0.1
0
0.1
0.2
0.3
0.4
0.5
0.6
0.7
0.8
0.9
1.0
1.1
1.2
1.3

2. the buildup to the maximum in the equatorial plane beyond the plasma is extremely gradual.

The current distribution (φ component) is

$$j_\varphi = j_0 e^{-\alpha_1\left(\frac{r}{R}\right)^2}\left\{\left(\frac{r}{R}\right)^{-1}\frac{1}{\beta \sin\theta}\left(e^{-\beta\cos^2\theta} - e^{-\beta}\right)\left[\left(1-2\alpha_1\left(\frac{r}{R}\right)^2\right)\left(1-e^{-\Delta\left(\frac{r}{R}\right)^2}\right) + 2\Delta\left(\frac{r}{R}\right)^2 e^{-\Delta\left(\frac{r}{R}\right)^2}\right] - \frac{1}{\alpha_1}\left(\frac{r}{R}\right)^{-3}\left(2\beta\cos^2\theta + \sin\theta\right) e^{-\beta\cos^2\theta}\left(1+\frac{\alpha_1}{\alpha_1+\Delta}e^{-\Delta\left(\frac{r}{R}\right)^2}\right)\right\}, \tag{6}$$

where $\Delta = \alpha_2 - \alpha_1$. These currents are distributed throughout a region containing the equatorial plane, and hence must flow inside the plasma rather than near its surface, producing the strong fields inside. However, if β is assumed to be very large, in essence driving the currents into the equatorial plane, further comparison with the experimental results can be made. Experimentally, currents were described in terms of a linear current density,

$$di = j'dr. \tag{7}$$

Equation (6) describes a surface density of current,

$$d^2i = \vec{j}\cdot d\vec{A} = j_\varphi r d\theta dr, \tag{8}$$

as shown in Figure 9. Therefore, a comparison is justified between the experimental linear current density and

$$j' = \int_0^\pi j_\varphi r\, d\theta. \tag{9}$$

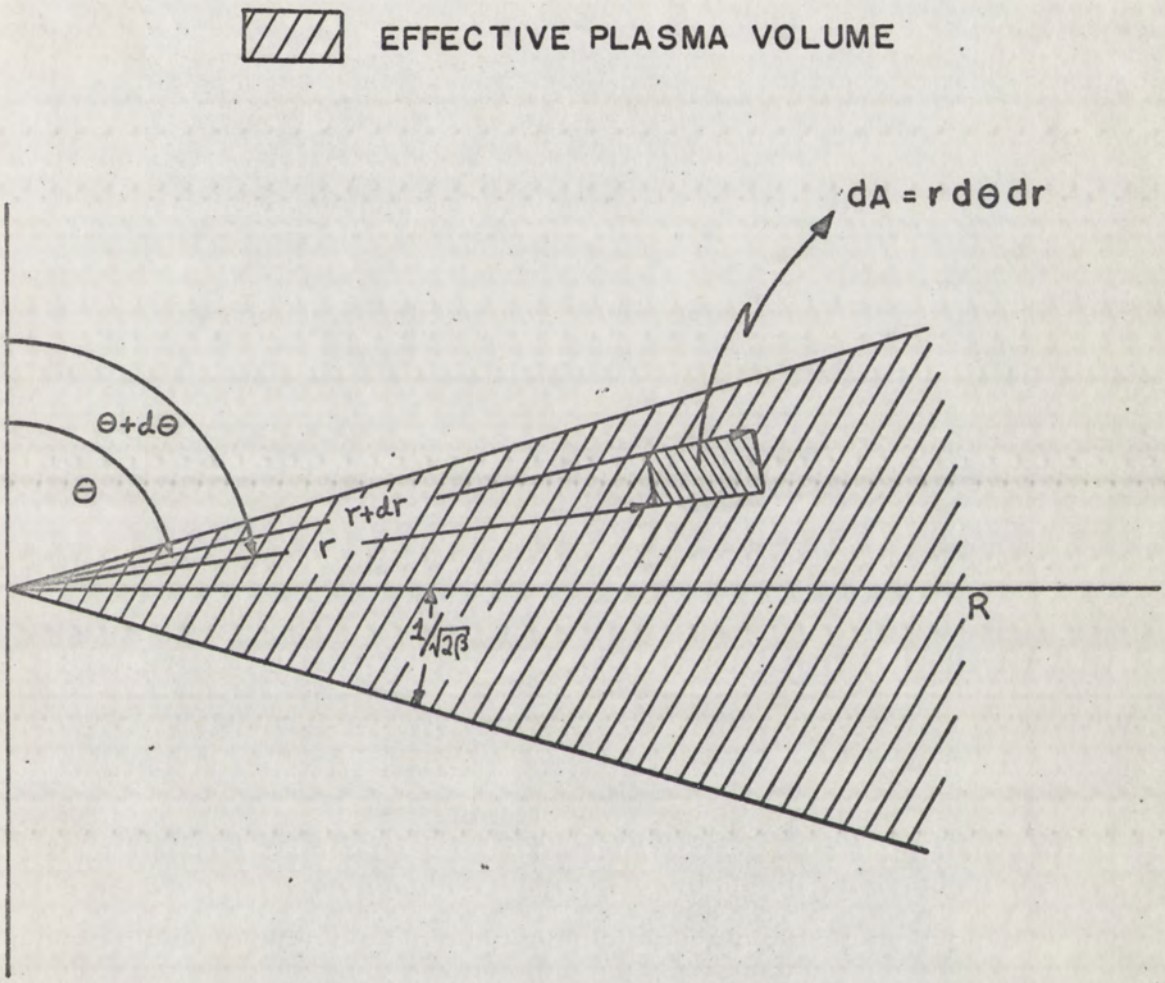

FIGURE 9
EFFECTIVE CROSS SECTION OF PLASMA
(FOR INTEGRATION OF CURRENT DISTRIBUTION (6))

For a large β, the currents are essentially confined to the region shaded in Figure 9. Using these approximations, integration of (9) over θ gives

$$j' = j_o e^{-\alpha_1 \left(\frac{r}{R}\right)^2} \frac{1}{\alpha_1} \sqrt{\frac{\pi}{\beta}} \left[1 + \frac{\alpha_1}{\alpha_1 + \Delta} e^{-\Delta \left(\frac{r}{R}\right)^2} \right] \left(\frac{r}{R}\right)^{-2}, \qquad (10)$$

with higher-order terms contributing no more than a few percent for $\beta > 20$. For r small compared to R, this resulting linear current density approximates the $1/r^2$ dependence observed experimentally.

The apparent basic flaw in these models is that the currents flow throughout the plasma rather than near its surface only. A representation was suggested, therefore, in which the currents flow in essence on the boundary of a torus. The magnetic field, shown in Figure 10, has the components

$$H_r = H_o \left(\frac{r}{R}\right)^{-2} \cot\theta \; e^{-\beta\left(\frac{r}{R} - \sin\theta\right)^2}, \qquad (11a)$$

and

$$H_\theta = H_o \left(\frac{r}{R}\right)^{-1} \frac{1}{\sin\theta} \left[e^{-\beta\left(\frac{r}{R} - \sin\theta\right)^2} - e^{-\beta\left(\frac{r}{R}\right)^2} \right], \qquad (11b)$$

where β again represents the angular spread of the current distribution. In the vicinity of the origin, a shape is observed which appears similar to the particle density contours of the Van Allen belts. This behavior

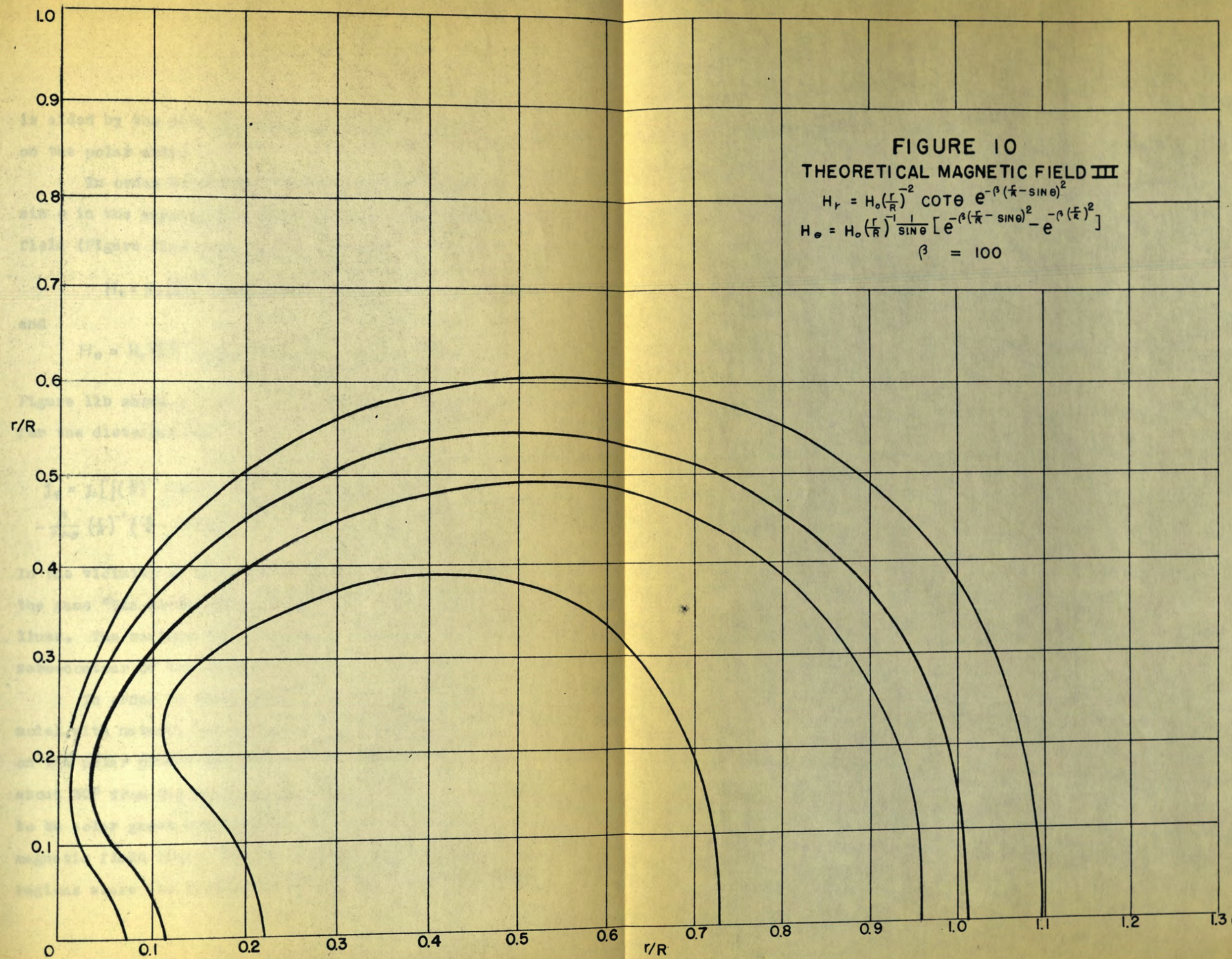

FIGURE 10

THEORETICAL MAGNETIC FIELD III

$$H_r = H_o\left(\frac{r}{R}\right)^{-2} \cot\theta \; e^{-\beta\left(\frac{r}{R} - \sin\theta\right)^2}$$

$$H_\theta = H_o\left(\frac{r}{R}\right)^{-1} \frac{1}{\sin\theta}\left[e^{-\beta\left(\frac{r}{R} - \sin\theta\right)^2} - e^{-\beta\left(\frac{r}{R}\right)^2}\right]$$

$$\beta = 100$$

is aided by the condition that the θ component vanish on the polar axis.

In order to elongate the plasma, the power of $\sin\theta$ in the exponential was raised to 2. The magnetic field (Figure 11a) then has the components

$$H_r = H_0 \left(\frac{r}{R}\right)^{-2} \cos\theta \; e^{-\beta\left(\frac{r}{R} - \sin^2\theta\right)^2}, \tag{12a}$$

and

$$H_\theta = H_0 \left(\frac{r}{R}\right)^{-1} \frac{1}{2\sin\theta} \left[e^{-\beta\left(\frac{r}{R} - \sin^2\theta\right)^2} - e^{-\beta\left(\frac{r}{R}\right)^2} \right]. \tag{12b}$$

Figure 11b shows a plot of iso-current density lines for the distribution

$$j_\varphi = j_0 \left[\left\{ \left(\frac{r}{R}\right)^{-3} \sin\theta \left[1 - 4\beta \cos^2\theta \left(\frac{r}{R} - \sin^2\theta\right) \right] - \frac{\beta}{\sin\theta} \left(\frac{r}{R}\right)^{-1} \left(\frac{r}{R} - \sin^2\theta\right) \right\} e^{-\beta\left(\frac{r}{R} - \sin^2\theta\right)^2} + \frac{\beta}{\sin\theta} e^{-\beta\left(\frac{r}{R}\right)^2} \right]. \tag{13}$$

In the vicinity of the origin, these lines follow much the same "Van Allen belt" contour as the magnetic field lines. The maximum field intensity is found at the zero-contour of the current density.

In order to investigate the correspondence of this model with nature, use was made of observational data on the polar plumes mentioned earlier, which appear about 30° from the poles of the sun. If these are assumed to be solar gases constrained to the contour of the magnetic field lines, then they must appear in those regions where the strongest field leaves the solar surface.

FIGURE 11a

THEORETICAL MAGNETIC FIELD IV

$$H_r = H_o \left(\frac{r}{R}\right)^{-2} \cos\theta \; e^{-\beta\left(\frac{r}{R} - \sin^2\theta\right)^2}$$

$$H_\theta = H_o \left(\frac{r}{R}\right)^{-1} \frac{1}{2\sin\theta} \left[e^{-\beta\left(\frac{r}{R} - \sin^2\theta\right)^2} - e^{-\beta\left(\frac{r}{R}\right)^2}\right]$$

$$\beta = 100$$

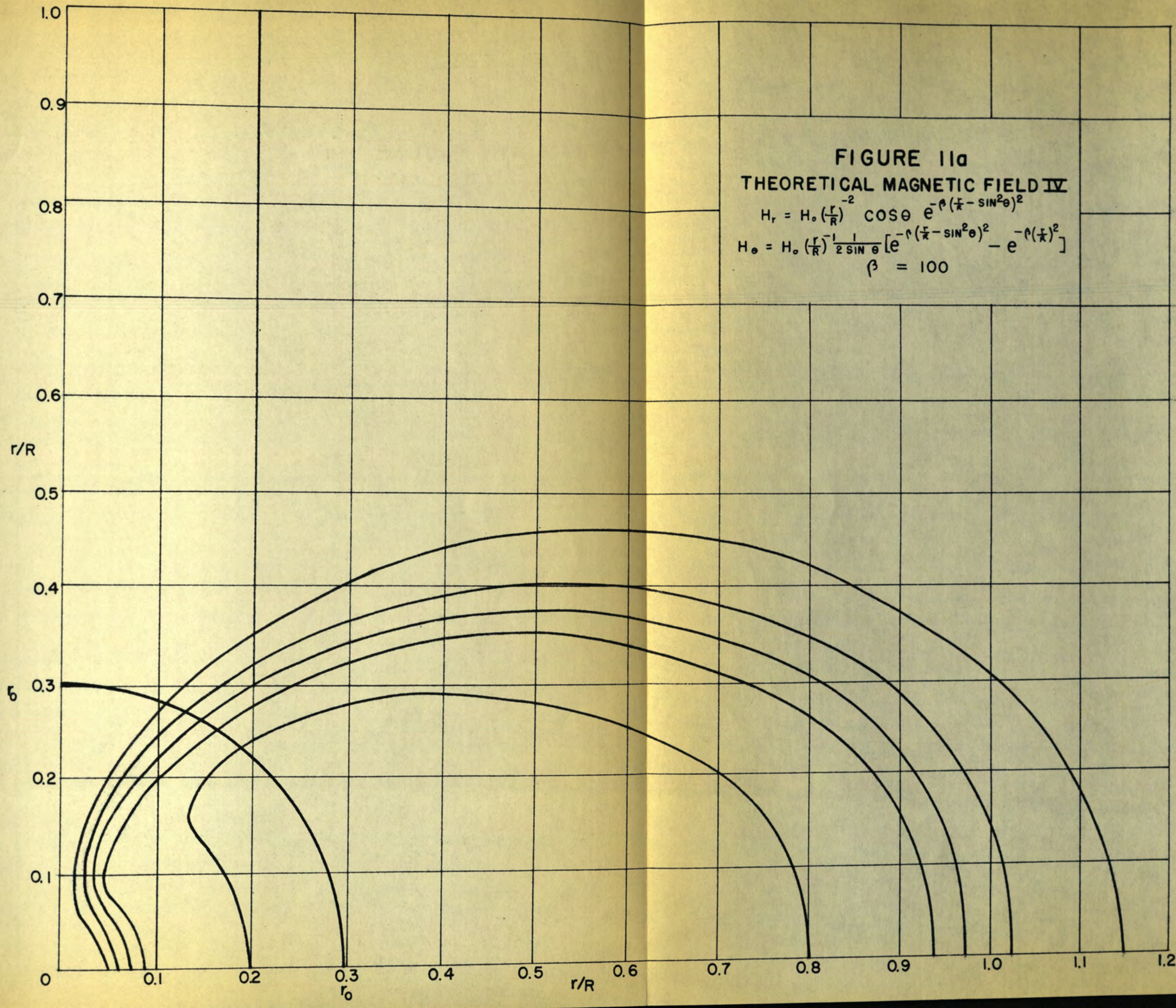

FIGURE IIb

THEORETICAL CURRENT DENSITY IV

$$J_\varphi = J_o\left[\left\{\left(\frac{r}{R}\right)^{-3}\sin\theta\left[1-4\beta\cos^2\theta\left(\frac{r}{R}-\sin^2\theta\right)\right]-\frac{\beta}{\sin\theta}\left(\frac{r}{R}\right)^{-1}\left(\frac{r}{R}-\sin^2\theta\right)\right\}e^{-\left(\frac{r}{R}-\sin^2\theta\right)^2}+\frac{\beta}{\sin\theta}\,e^{-\beta\left(\frac{r}{R}\right)^2}\right]$$

····· CURRENTS INTO PAPER

×××× CURRENTS OUT OF PAPER

—— NEUTRAL CONTOUR

=·=·= CONTOURS OF MAXIMUM CURRENTS

NUMBERS REPRESENT H/H_o

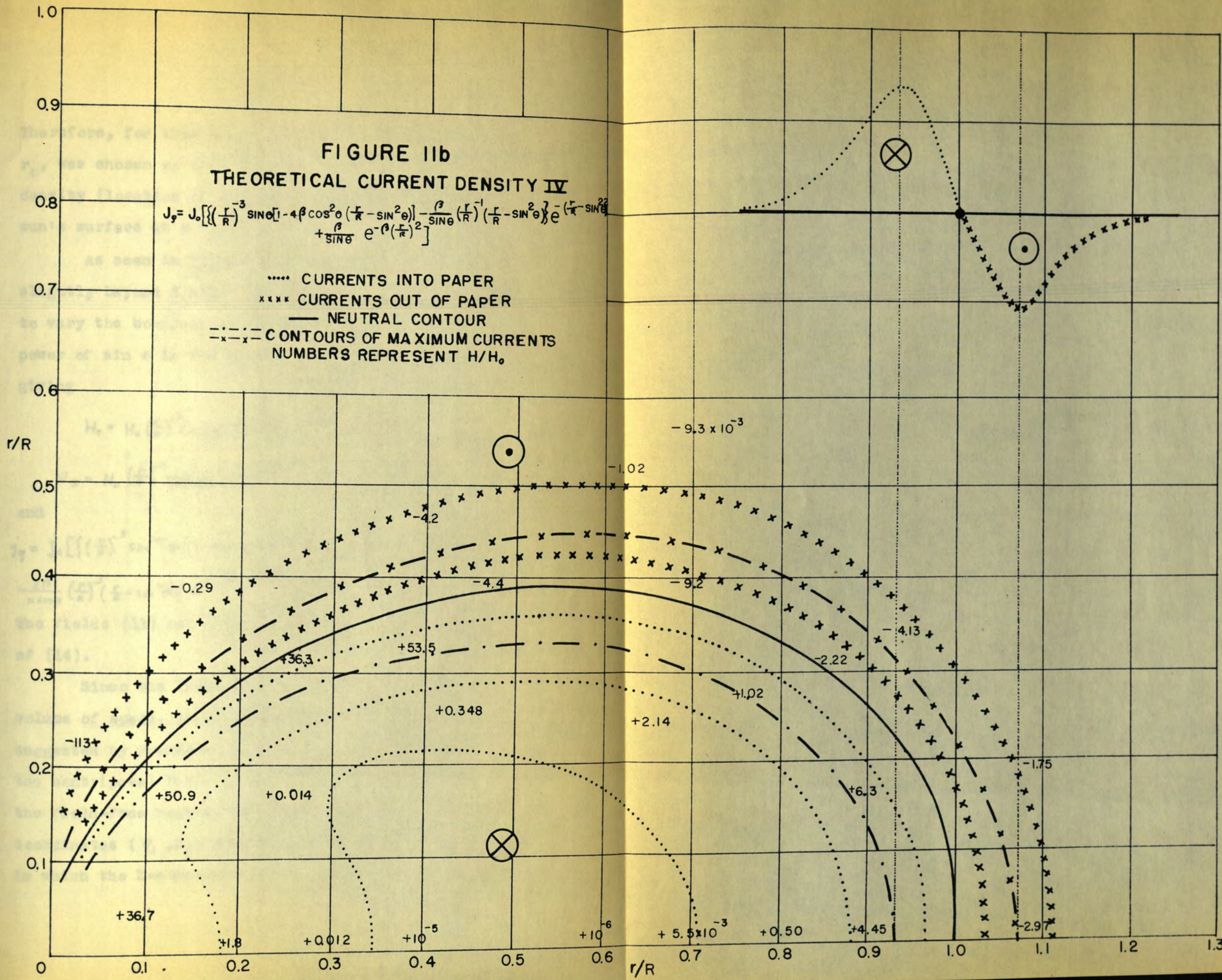

Therefore, for this model, the effective solar radius, r_0, was chosen so that the neutral surface of the current density (location of the maximum field) intersects the sun's surface at $\theta = 30^0$.

As seen in Figure 11a, the plasma extends only slightly beyond 3 solar radii for this model. In order to vary the boundary of the plasma relative to r_0, the power of sin θ in the exponential was made arbitrary, giving

$$H_r = H_0 \left(\frac{r}{R}\right)^{-2} \cos\theta \sin^{N-2}\theta \; e^{-\beta\left(\frac{r}{R} - \sin^N\theta\right)^2}, \qquad (14a)$$

$$H_\theta = H_0 \left(\frac{r}{R}\right)^{-1} \frac{1}{N\sin\theta} \left[e^{-\beta\left(\frac{r}{R} - \sin^N\theta\right)^2} - e^{-\beta\left(\frac{r}{R}\right)^2}\right], \qquad (14b)$$

and

$$j_\varphi = j_0 \left[\left\{\left(\frac{r}{R}\right)^{-3} \sin^{N-1}\theta \left[1 - (N-2)\cot^2\theta - 2N\beta\cos^2\theta \sin^{N-2}\theta \left(\frac{r}{R} - \sin^N\theta\right)\right] - \frac{2\beta}{N\sin\theta}\left(\frac{r}{R}\right)^{-1}\left(\frac{r}{R} - \sin^N\theta\right)\right\} e^{-\beta\left(\frac{r}{R} - \sin^N\theta\right)^2} + \frac{2\beta}{N\sin\theta} e^{-\beta\left(\frac{r}{R}\right)^2}\right]. \qquad (14c)$$

The fields (11) and (12) are seen to be special cases of (14).

Since the field can now be confined to a small volume of space, it is possible to use a procedure suggested by Professor T. Gold for a determination of the centripetal force on the plasma contained within the field-free region. In Figure 12, the cylindrical coordinates (ϱ_1, Z_1) describe the center of the region in which the Z-component of the magnetic field vanishes.

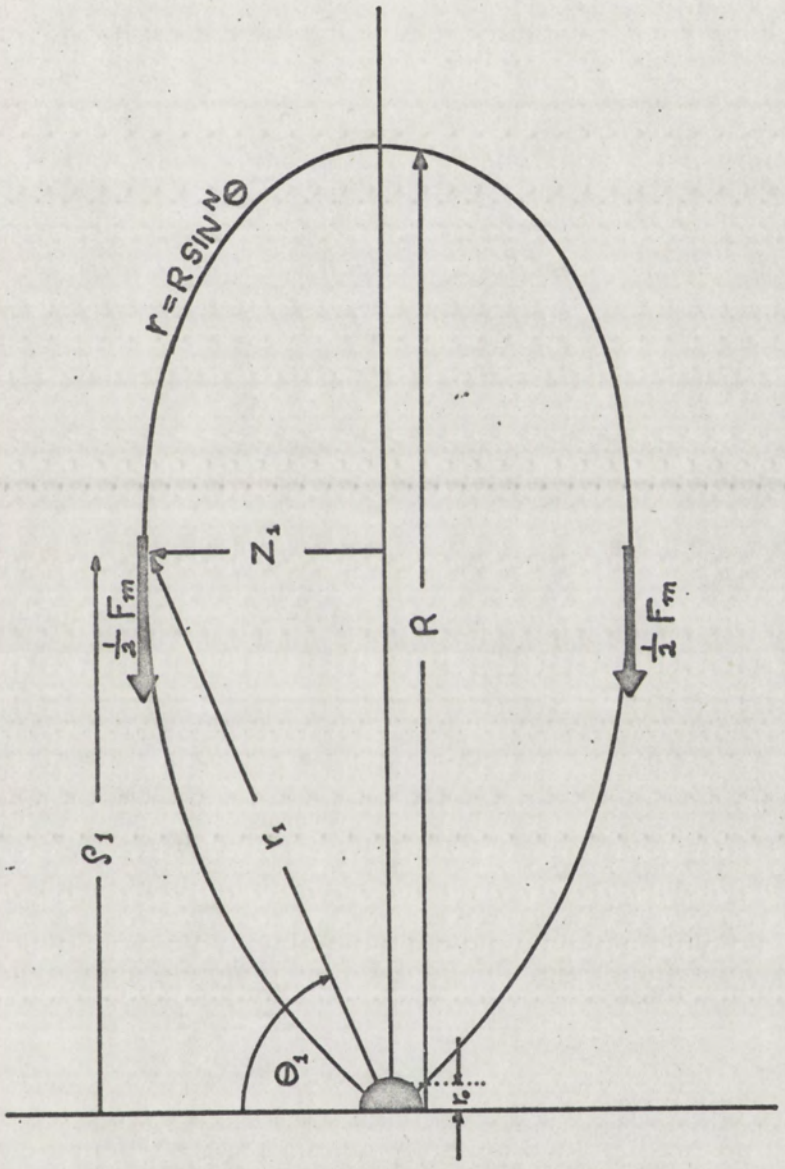

FIGURE 12

CENTRIPETAL FORCE EXERTED ON PLASMA BY MAGNETIC FIELD

The magnetic pressure at any point is given by the energy density,

$$P = H^2/8\pi . \qquad (15)$$

Integrating (15) over the cylindrical surface of radius ς_1, one obtains the force exerted by the magnetic field on the plasma,

$$F_m = \varsigma_1/2 \int H^2 dZ, \qquad (16)$$

where

$$\frac{\varsigma_1}{r_0} = 2^N \left(\frac{N}{N+1}\right)^{\frac{N+1}{2}} . \qquad (17)$$

A field of 1 gauss is assumed at $\theta = 30^\circ$ on the sun's surface.

To find the centrifugal force of the rotating plasma, consider the thin cylindrical slab of plasma shown in cross-section in Figure 13. Assuming an ideal gas at constant temperature $T = 10^6$ degrees, the pressure at any point is then given by

$$P = n(\varsigma)kT. \qquad (18)$$

The number density n is given as a function of ς since, due to lack of further data, values of n known in the equatorial plane are assumed to hold also at the distance Z_n in the plane normal to the equatorial plane.

The pressure (18) produces on each unit area of the surface of the slab a force normal to the surface.

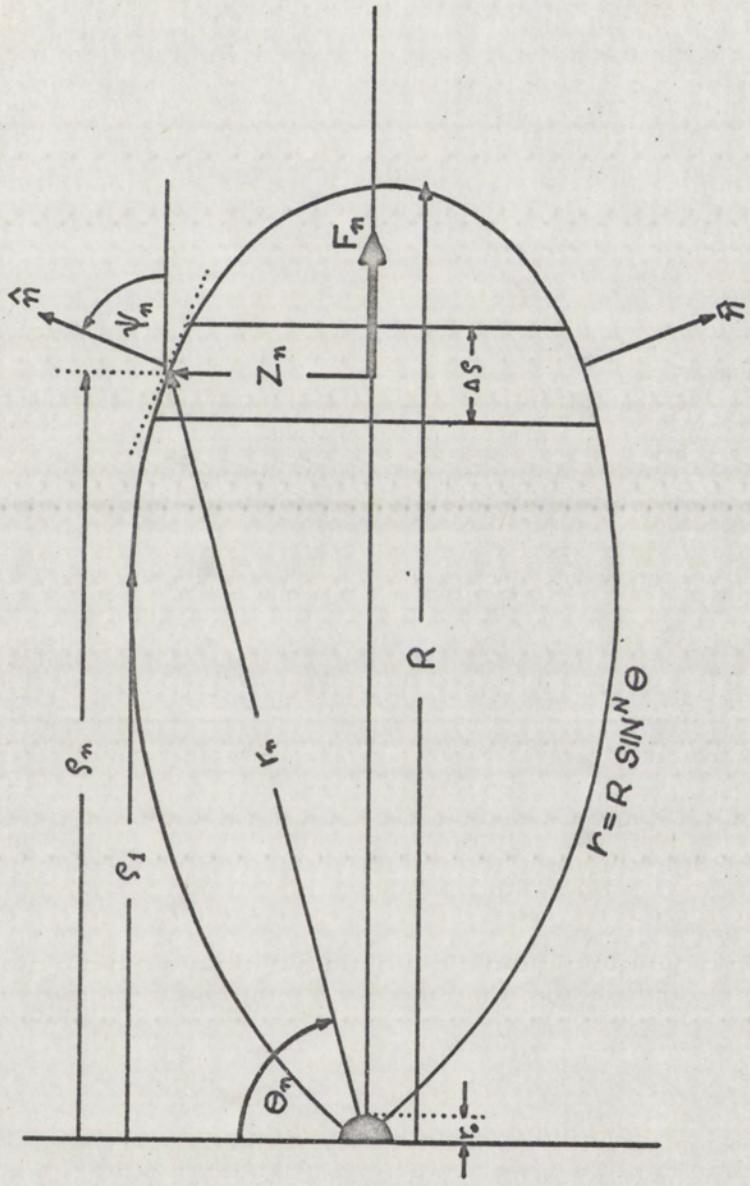

FIGURE 13
CENTRIFUGAL FORCE OF ROTATING PLASMA

Integrating this pressure over the surface of the slab, one obtains the total force exerted on the slab,

$$F_n = 2\pi Z_n \frac{\Delta\rho}{\sin\psi_n} n(\rho) kT \cos\psi_n, \qquad (19)$$

where ψ_n, the angle made by the outward normal to the field and the horizontal, is given by

$$\cot\psi_n = \frac{\tan\theta_n - N\cot\theta_n}{N+1}, \qquad (20)$$

and

$$\sin\theta_n = \left(\frac{\rho_n}{R}\right)^{\frac{1}{N+1}}. \qquad (21)$$

Summing (19) over all such slabs from the synchronous orbit to the boundary of the plasma, one obtains the total particle force,

$$F_p = \sum 2\pi Z_n \Delta\rho\, nkT \cot\psi_n, \quad \rho_1 \leq \rho_n \leq R. \qquad (22)$$

By varying the parameter N, it was found possible to establish, by trial and error, equilibrium between the forces only if the co-rotating plasma did not extend farther than 44 solar radii. The magnetic field for which equilibrium was found is shown in Figure 14a. The same field is plotted in the vicinity of the origin in Figure 14b, showing most of the "Van Allen belt" behavior to be contained within the effective solar surface.

FIGURE 14a

THEORETICAL MAGNETIC FIELD V

$$H_r = H_o\left(\frac{r}{R}\right)^{-2} \cos\theta \sin^{N-2}\theta \; e^{-\beta\left(\frac{r}{R} - \sin^N\theta\right)^2}$$

$$H_\theta = H_o\left(\frac{r}{R}\right)^{-1} \frac{1}{N \sin\theta}\left[e^{-\beta\left(\frac{r}{R} - \sin^N\theta\right)^2} - e^{-\beta\left(\frac{r}{R}\right)^2}\right]$$

$N = 5.5 \qquad \beta = 10^3$

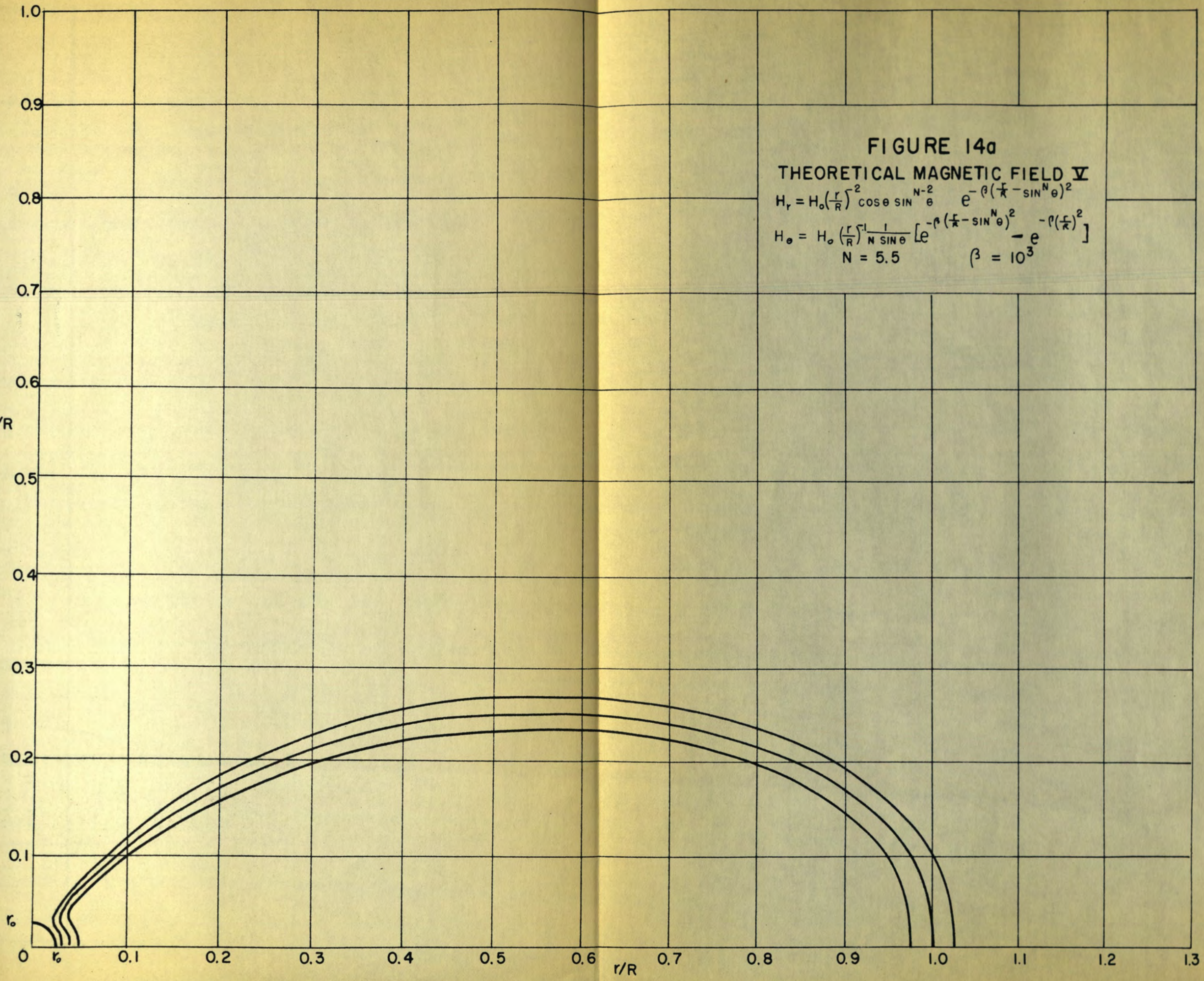

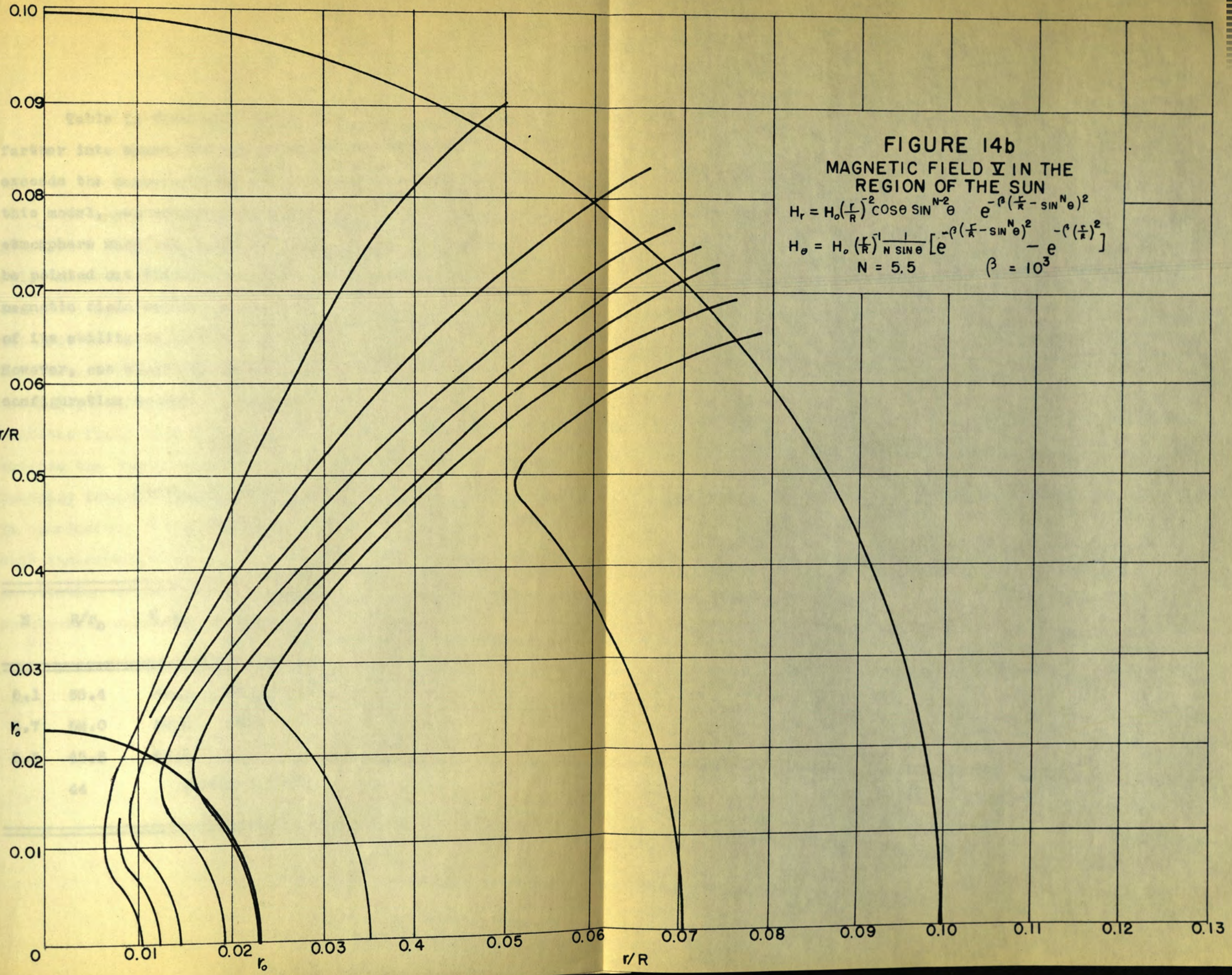

FIGURE 14b

MAGNETIC FIELD $\mathbf{V}$ IN THE REGION OF THE SUN

$$H_r = H_o\left(\frac{r}{R}\right)^{-2}\cos\theta \sin^{N-2}\theta \quad e^{-\beta\left(\frac{r}{R} - \sin^N\theta\right)^2}$$

$$H_\theta = H_o\left(\frac{r}{R}\right)^{-1}\frac{1}{N\sin\theta}\left[e^{-\beta\left(\frac{r}{R} - \sin^N\theta\right)^2} - e^{-\beta\left(\frac{r}{R}\right)^2}\right]$$

$N = 5.5 \qquad \beta = 10^3$

Table II shows that for plasma volumes extending farther into space, the particle force (20) rapidly exceeds the magnetic force (19). Thus, on the basis of this model, one cannot expect co-rotation of the solar atmosphere much beyond the synchronous orbit. It should be pointed out that this model, with a rather thin magnetic field region, is very favorably shaped in terms of its ability to enforce co-rotation beyond 40 solar radii. However, one would not really expect such an extreme configuration to occur in nature.

TABLE II

FORCES ON THE SOLAR PLASMA

($\beta = 10^3$)

N	R/r_o	ρ_1/r_o	Z_1/r_o	$F_p \times 10^{18}$ Dynes	$F_m \times 10^{17}$ Dynes	F_p/F_m
6.1	68.4	40.0	16.1	8.64	9.42	9.2
5.7	52.0	30.2	12.6	4.10	9.85	4.2
5.5	45.3	26.3	11.2	2.08	12.9	1.6
	44		(EXTRAPOLATED)			1

CHAPTER IV

CONCLUSION

An experimental model was constructed which provided a rough approximation to the behavior of the solar magnetic field at large distances from the sun. In addition, several theoretical models were investigated. The last one contained sufficient flexibility in the form of arbitrary parameters to permit adjustment to known physical data. The currents producing such a magnetic field flow in opposite directions inside and outside the boundary, with a neutral surface at the boundary itself, where the magnetic field is largest. In conclusion, it was determined that on the basis of both the experimental and the theoretical models, co-rotation of the solar atmosphere much beyond the synchronous orbit is not likely.